

*Spectroscopic study of the system  $^2\Sigma \rightarrow ^2\Pi$  of OH-radical and determination of the rotational temperatures by using a numerical model.*

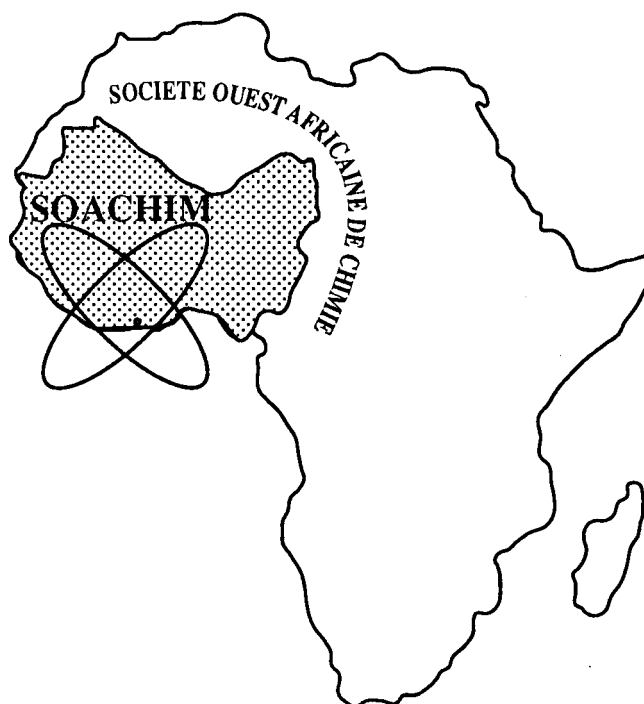
**Samuel Ouoba, Tizane Daho, Arsène H. Yonli,**

**Jean Kouliati**

*Journal de la Société Ouest-Africaine de Chimie*

*J. Soc. Ouest-Afr. Chim.(2014), 038 : 22- 29*

19<sup>ème</sup> Année, Décembre 2014



ISSN 0796-6687

Code Chemical Abstracts : JSOCF2  
Cote INIST (CNRS France) : <27680>  
Site Web: <http://www.soachim.org>

## **Spectroscopic study of the system ${}^2\Sigma \rightarrow {}^2\Pi$ of OH-radical and determination of the rotational temperatures by using a numerical model.**

**Samuel Ouoba\*, Tizane Daho, Arsène H. Yonli, Jean Kouliati**

*Laboratoire de Physique et de Chimie de l'Environnement, Université de Ouagadougou, UFR-SEA, 03 BP 7021 Ouaga 03, Burkina Faso.*

(Reçu le 03/03/2014 – Accepté après corrections le 20/12/ 2014)

**Abstract:** We develop in this note a simple and practical method for the determination of the rotational temperatures based on the observation of molecular bands produced by the OH-radical. For this, we make an approach based on the concept of thermodynamic equilibrium and we proceed to a detailed study of OH. We carry out the simulation of this OH-radical by systematically assuming the different cases of Hund. We have revised the molecular constants of the literature related to OH-radical, and we have used the expressions of the rotational energy levels which are in good agreement with literature data. We have established the evolution of the rotational structures as a function of the simulation parameters. The comparison between the results of literature and the simulated results has allowed deducing the rotational temperatures by using Boltzmann method.

**Keywords:** Energy Levels; Spectrum; Rotational Temperature; OH-radical; Numerical Model.

## **Etude spectroscopique du système ${}^2\Sigma \rightarrow {}^2\Pi$ du radical OH et détermination des températures de rotation en utilisant un modèle numérique.**

**Résumé :** Nous développons dans cet article une méthode simple et pratique pour la détermination des températures de rotation à partir des spectres produits par le radical OH. Pour cela, nous faisons une approche basée sur l'équilibre thermodynamique et nous procédons à une étude détaillée du radical OH. Nous élaborons ensuite un modèle de simulation en se référant aux différents cas de Hund. Nous passons également en revue les constantes moléculaires disponibles dans la littérature sur le radical OH et nous utilisons des expressions pour les niveaux d'énergies qui sont en bon accord avec les résultats de la littérature. Nous avons pu établir que l'évolution des structures rotationnelles est fonction des paramètres du modèle de simulation. La comparaison entre les résultats de la littérature et ceux du modèle a permis de déduire les températures rotationnelles en utilisant la méthode de Boltzmann.

**Mots clés :** Niveaux d'Energie ; Spectre ; Température Rotationnelle ; Radical OH ; Modèle Numérique.

---

\* **Corresponding author** : E-mail address : samuel\_ouoba1@yahoo.fr (Samuel Ouoba)

## 1. Introduction

Spectroscopic analysis of the radiation emitted by plasma is an excellent way of diagnostic because it does not disturb the plasma as it is the case where different kinds of probes are used. The only drawback is the inability to detect the non-radiative states. To determine the rotational temperature of the plasma, several methods are proposed, such as Boltzmann graph method, the method of measuring the absolute intensity or the relative intensity. In certain regions of plasma with low temperature where the electronic density decreases significantly, the intensity of atomic radiation is very low and the measurement errors of the temperature become increasingly important. In most of plasma and for certain ranges of temperature, we can observe some molecular spectra of OH-radical highly developed. Indeed, OH-radical plays a key role in atmospheric chemistry from the surface through the mesosphere. Its distribution in the 30–70 km altitude region of the atmosphere is important in determining global stratospheric temperatures and circulation through its influence on the ozone budget<sup>[1]</sup>. The formation and destruction of ozone in the upper stratosphere and lower mesosphere is controlled mainly by reactions involving odd-hydrogen species, so the understanding of these reactions is crucial to the study of radiative and climatic effects of ozone change<sup>[2]</sup>. The accuracy of model calculations that describe the coupling between ozone and OH radicals has improved significantly in recent years with the availability of satellite data<sup>[3]</sup>. Vertical concentration profiles of OH have been retrieved from measurements by satellite instruments including the Aura Microwave Limb Sounder (MLS) and Middle Atmosphere High Resolution Spectrograph Investigation (MAHRSI)<sup>[4; 5]</sup>. About emission spectra and rotational temperature measurement, several recent methods have been used in the literature. We can name the high efficiency terahertz (THz) sources of Drouin<sup>[6]</sup>, the R2PI Spectroscopy used by Carpentier<sup>[7]</sup>, Cavity Ring-Down (CRD) Spectroscopy used by Tanner<sup>[8]</sup>, the sub-Doppler infrared spectroscopy in a slit supersonic discharge expansion source of Buckingham<sup>[9]</sup>. We can also add other many methods such as the one of Dehghani<sup>[10]</sup> using dry ice cooled gas cell, the technical of Siller<sup>[11]</sup> based on optical parametric oscillator calibrated with an optical frequency comb and many other methods<sup>[12–15]</sup>.

Among all these methods encountered in the literature, no one uses, for the radical OH, a numerical model to determine emission spectra and

rotational temperature. That is the main originality of the present paper which is an essential contribution in the understanding of the behavior of plasma containing OH-radical. For this, we have determined first the main variables of OH-radical such as the lines strengths and the wavelengths corresponding to the three branches *P*, *Q* and *R* studied. In a second approach we have investigated the influence of the device profile and we have determined the head of the branches sensitive to the temperature of rotation. Finally, Boltzmann method is used to determine rotational temperature with the model. Comparison of our results with those of literature shows that the model proposed in this paper gives results in good agreement with experimental results and can possibly be applied to other molecules.

## 2. Materials and Methods

The interest and the originality of the numerical model presented in this paper are useful for several reasons. Firstly it allows the identification of the compounds. Secondly, the model allows us to easily determine the rotational temperature by comparing the simulated and the experimental data of intensities and the positions of the rotational stripes. For this, the simulation process we have adopted is based on the following steps:

- We determine the spectral terms of rotation of each state and each doublet, taking into account the splitting of the spin, the *A*-doubling, and, the term taking into account the strong rotations,
- We determine the wavelengths of the branches *P*, *Q* and *R* considering the specific selection rules of each branch,
- We establish the terms of the lines strengths,
- We identify the different molecular constants,
- We define a scale (spectral resolution) in order to integrate the intensities of all the stripes having their wavelengths in the same interval. The representation of the integrated intensities as a function of wavelength is called an ideal spectrum. The graphical representation obtained is a Dirac comb where each peak has its own intensity.

The device profile plays an important experimental role. In most cases, a slot of spectral apparatus gives a Gaussian spectral profile with a half - width, *DX*, at 1/e of height. This half - width is an essential parameter of the simulation program. Finally, we proceed to the numerical convolution of each Dirac peak with the Gaussian profile and we get the final simulated spectrum whose parameters are *DX* and *T<sub>r</sub>*.

### 3. Basic Formulas

#### 3.1. Rotational energy, term of energy and wave numbers

Considering that the resulting of the orbital angular momentum  $L \neq 0$ , we can obtain the rotational energy using respectively case (a) and case (b) of Hund:

$$E_r = BJ(J + 1) \quad (1)$$

$$E_r = B[K(K + 1) - L^2] \quad (2)$$

The rotational energies used for  ${}^2\Sigma$  (Equations 3a and 3b) and  ${}^2\pi$  (Equations 4a and 4b) are respectively defined by:

$$F_1(K) = BK(K + 1) - DK^2(K + 1)^2 + R(K + 1/2) \quad (3a)$$

$$F_2(K) = BK(K + 1) - DK^2(K + 1)^2 - R(K + 1/2) \quad (3b)$$

$$f_1(K) = B \left[ (K + 1)^2 - 1 - \frac{1}{2} \sqrt{4(K + 1)^2 + a(a - 4)} \right] - DK^2(K + 1)^2 \text{ with } J - \frac{1}{2} = K \quad (4a)$$

$$f_2(K) = B \left[ K^2 - 1 + \frac{1}{2} \sqrt{4K^2 + a(a - 4)} \right] - DK^2(K + 1)^2 \text{ with } J + \frac{1}{2} = K \quad (4b)$$

For both states ( $\Sigma$  and  $\pi$ ), the constants  $B$ ,  $D$  and  $R$  are characteristic of the state and  $a$  is called coupling constant. If we take into account the  $L$ -doubling, we can establish two supplementary levels of energies named by  $f_1'(K)$  and  $f_2'(K)$  and given by:

$$f_1'(K) - f_1(K) = b_1 K(K + 1) \quad (5a)$$

$$f_2'(K) - f_2(K) = b_1 K(K + 1) \quad (5b)$$

Where  $b_1$  is a constant depending to the state.

The Three branches named  $P$ ,  $Q$  and  $R$  obey to the transition rules characterized by  $\Delta K=0$  or  $\Delta K=\pm 1$  and are called strong branches. The other branches characterized by two indices and denoted by  $P_{ij}$ ,  $Q_{ij}$ ,  $R_{ij}$  with  $i, j = 1, 2$  and  $i \neq j$  are called satellite branches or weak branches. Taking into account only the strong branches, we obtain ten branches also called wave numbers which can be expressed as a function of the energy of the initial state and the final state levels<sup>[16]</sup>:

#### 3.2. The lines strengths

The lines strengths also called transition probabilities depend essentially on the quantum number of rotation  $J$  and the coupling constant  $a$ .

They can be determined using the expressions of the energies levels and are given by:

$$R_2 = \frac{2J+1}{2J+2} \{ (2J + 1) + U[(2J + 1)^2 - 2a] \} \quad (6)$$

$$\begin{cases} R_1 \\ Q_{12} \end{cases} = \frac{2J+1}{2J+2} \{ (2J + 1) \pm U[(2J + 1)^2 + 2(a - 4)] \} \quad (7)$$

$$\begin{cases} Q_2 \\ R_{21} \end{cases} = \frac{2J+1}{2J+2} \left\{ \frac{(2J+1)^2 - a \pm U[(2J+1)^2 - 8J - 2a]}{J} \right\} \quad (8)$$

$$\begin{cases} Q_1 \\ P_{12} \end{cases} = \frac{2J+1}{2J+2} \left\{ \frac{(2J+1)^2 - 2 \pm U[(2J+1)^2 - 8J + 2(a - 4)]}{J} \right\} \quad (9)$$

$$P_1 = \frac{2J+1}{2J} \{ (2J + 1) + U[(2J + 1)^2 - 2a] \} \quad (10)$$

$$\begin{cases} P_2 \\ Q_{21} \end{cases} = \frac{2J+1}{2J} \{ (2J + 1) \pm U[(2J + 1)^2 + 2(a - 4)] \} \quad (11)$$

Where  $U$  is given by:

$$U^{-1} = \sqrt{(2J + 1)^2 + a(a - 4)} \quad (12)$$

In equations 6 to 11, the sign (+) before the  $U$  is always refers to the main branches and the sign (−) refers to the satellite branches. Considering the nature of the transitions  $\Sigma$  and  $\pi$ , the molecular constants of OH-radical which appear in equations 1 to 12 are given in the **Table 1**.

## 4. Results and Discussion

### 4.1. Different parts of a simulated spectrum

We present in **Figure 1** the results of a simulated spectrum of OH in the spectral range between  $\lambda=3064.8 \text{ \AA}$  and  $\lambda=3331 \text{ \AA}$ .

The analysis of the numerical spectrum shows clearly that the rotational stripes of the different branches of OH-radical are distributed between five spectral intervals defined by:

- From  $\lambda=3064.8 \text{ \AA}$  to  $\lambda=3079.3 \text{ \AA}$  we have only the branches  $R$ . We can clearly distinguish the head of the branch  $R$  for  $\lambda=3068.5 \text{ \AA}$ ,
- From  $\lambda=3079.3 \text{ \AA}$  to  $\lambda=3082.6 \text{ \AA}$  we have a superposition of the branches  $Q$  and  $R$ ,
- From  $\lambda=3082.6 \text{ \AA}$  to  $\lambda=3161.9 \text{ \AA}$  we have a superposition of all the three branches  $P$ ,  $Q$  and  $R$ . We can identify the head of the branch  $Q$  for  $\lambda=3090.7 \text{ \AA}$  which is a complex stripe well resolved,
- From  $\lambda=3161.9 \text{ \AA}$  to  $\lambda=3248.9 \text{ \AA}$  we have a superposition of the two branches  $Q$  and  $P$ ,
- From  $\lambda=3248.9 \text{ \AA}$  to  $\lambda=3331 \text{ \AA}$  we have only the branches  $P$ . It may be noted in that figure that the rotational stripe of the branches  $P$  are very low compared to the rest of the spectrum.

In contrast, the rotational stripes of the branches  $Q$  represent a major proportion of total rotational stripes of OH radical.

### 4.2. Influence of the rotational temperature

**Figure 2** is formed by the superposition of three simulated spectra normalized relatively to the head of the band *Q* with three values of rotational temperature i.e.  $T_r=3000$  K,  $5000$  K,  $7000$  K and for  $DX=1$ .

We can see that when the rotational temperature varies, the intensity of the head of the band *R*, normalized relatively to the intensity of the head of the band *Q* varies greatly. The rest of the spectrum varies also and some non-existent stripes at low temperatures become important with increasing temperature as for example the stripes of the branch

*P* which are nonexistent for  $T_r = 3000$  K and for wavelengths  $\lambda > 3260$  Å but become visible for  $T_r = 5000$  K and relatively large for  $T_r = 7000$  K. One of the important points is that the head of the band *R* is very sensitive to the temperature of rotation and can therefore serve as thermometer to evaluate the temperature of rotation.

### 4.3. Influence of device profile *DX*

The half - width *DX* to 1/e of height of the device of Gaussian profile is an important parameter for the simulation.

**Table 1:** Molecular constants of  ${}^2\Sigma \rightarrow {}^2\pi$ .

Constants	<i>B</i>	<i>D</i>	<i>R</i>	<i>a</i>	<i>b</i> <sub>1</sub>
State ${}^2\Sigma$	16.961	0.00204	0.1122	-	-
State ${}^2\pi$	18.515	0.00187	-	-7.547	0.0417

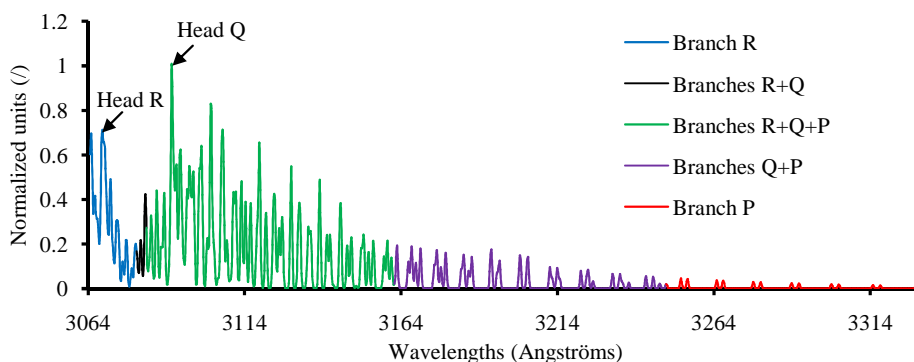


**Figure 1:** Simulated spectrum for  $T_r=4000$  K and  $DX=1/3$ .

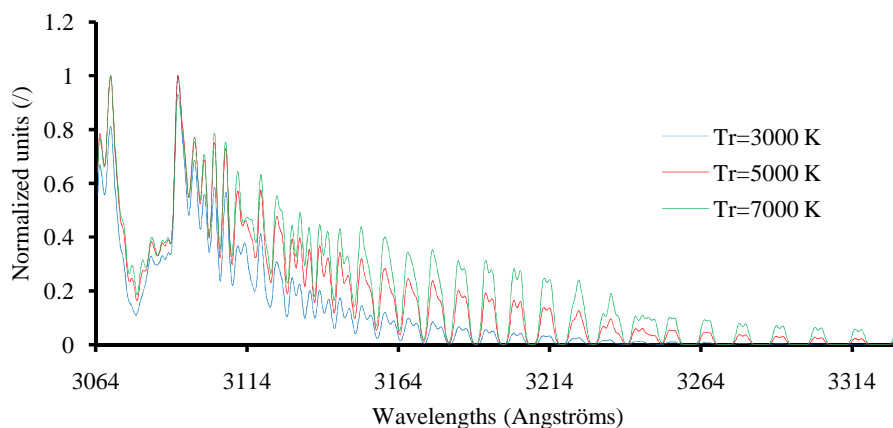


**Figure 2:** Superposition of three simulated spectra for three rotational temperatures.

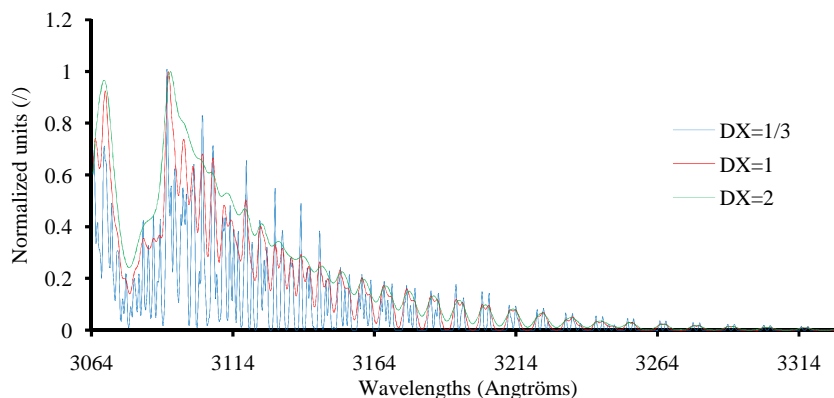


**Figure 3:** Superposition of three simulated spectra for three values of  $DX$ .

**Figure 3** is formed by the superposition of three spectra obtained for the same temperature  $T_r = 4000$  K and for three values of  $DX$  ( $DX = 1/3$ ,  $DX = 1$  and  $DX = 2$ ). We can see that when the value of the device profile  $DX$  is higher, the resolution of the spectrum is smaller because some recoveries can occur when the device function becomes important. Indeed  $DX$  allows us to define a level of spectral resolution by scanning the spectral band in an interval of given wavelengths in order to integrate the intensities of all the stripes which have their wavelengths in this interval. The representation of the integrated intensities of the stripes as a function of wavelength gives an ideal spectrum. That is why the rotational structure of the spectrum is destroyed when  $DX$  is increasing.

#### 4.4. Determination of the rotational temperatures by comparing simulated spectra and experimental spectra

We use in this section the Boltzmann method to determine the rotational temperatures using the

relative intensities of the thermometric and rotational stripes. This method was successfully used by Koulidiati <sup>[17]</sup> to evaluate the temperatures of rotation of CH and C<sub>2</sub>. Considering therefore the intensity of thermometer rotational stripe  $R$  we can obtain the following relation:

$$\ln \left( \frac{I_{J''V''}^{J'V'}}{S_{JJ''}} \right) = - \frac{hcF'(J)}{kT_r} \quad (13)$$

Where  $h$  is called Planck's constant,  $k$  is the Boltzmann's constant and  $c$  is the velocity of light. The intensity  $I_{J''V''}^{J'V'}$  is measured, the lines strengths  $S_{JJ''}$  and the high rotational energies level  $F'(J)$  are calculated. The expressing of energies levels is given by:

$$F'(J) = BJ(J + 1) \quad (14)$$

Three spectra experimentally validated (**Figures 4, 5 and 6**) obtained for three rotational temperatures have been selected for the validation of our simulation model <sup>[16]</sup>.

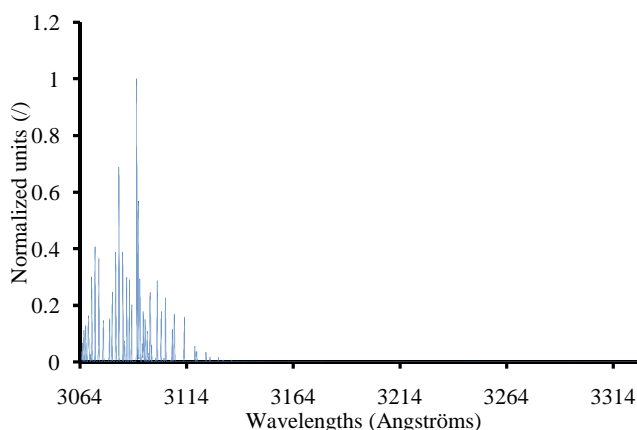


**Figure 4:** Literature data of the spectrum of the OH-radical for  $T_r=500$  K <sup>[16]</sup>.

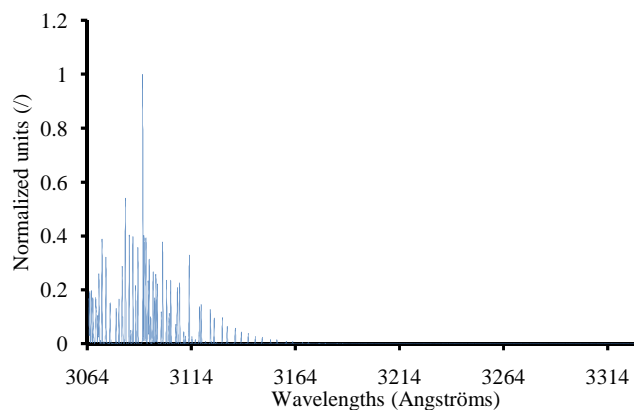


**Figure 5:** Literature data of the spectrum of the OH-radical for  $T_r=1000$  K <sup>[16]</sup>.

For the spectra of **Figures 4, 5** and **6**, the Boltzmann graphs are obtained using the simulation model. The linearity of the curves (**Figure 7**) shows that the populations of rotational levels of OH follow a distribution of Boltzmann and then we can define a temperature of rotation <sup>[18]</sup>. The use of the numerical model, by superposing numerical spectrum and experimental spectrum, allows us to determine the temperatures of rotation. **Table 2** presents the theoretical results about the rotation temperatures compared to the results of our model.

We can note that the results of the simulation model are in good agreement with the results of the literature. The three values of temperature are  $T_r=524$  K,  $T_r=1027$  K and  $T_r=2965$  K and the relative uncertainties for these three values of temperature are respectively 4.8%, 2.7% and 1.17%. The average uncertainty for the three values of rotational temperature is  $\Delta T=\pm 28.67$  K. Another

method based on Cavity Ring-Down laser Spectroscopy (CRDS) to measure the OH concentration profile has allowed to measure the rotational temperature with an uncertainty  $\Delta T=\pm 30$  K <sup>[19]</sup> that is in good agreement with the order of magnitude of uncertainties that we have obtained in this work.

For all the three theoretical spectra of OH studied, the use of our numerical model allows to obtain an expression for the rotational temperature  $T_r$  given by:

$$T_r = \frac{hc}{k \cdot \tan \varphi} \quad (15)$$

where  $\varphi$  is the value of the angle formed by the straight line of Boltzmann with the horizontal line. This relation has already been obtained by Lavrov and Otorbaev <sup>[17]</sup> for other molecules confirming that our model can be used to determine, with reasonable uncertainties, the rotational temperatures of OH in the range of wavelengths studied.

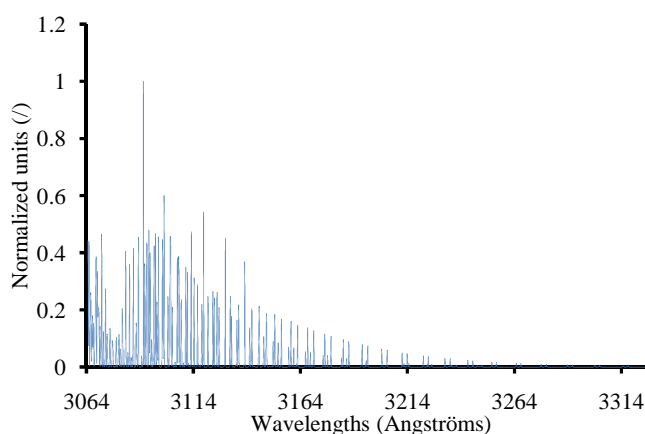


**Figure 6:** Literature data of the spectrum of the OH-radical for  $T_r=3000$  K <sup>[16]</sup>.

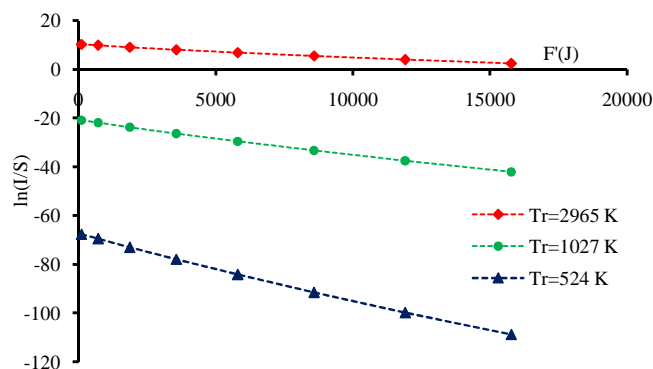


**Figure 7:** Determination of the rotational temperatures by using a numerical model.

**Table 2:** Comparison of rotational temperatures.

Results of literature <sup>[16]</sup>	Results of numerical model (This work)
$Tr=500$ K	$Tr=524$ K
$Tr=1000$ K	$Tr=1027$ K
$Tr=3000$ K	$Tr=2965$ K

## 5. Conclusion

In this manuscript, we have proposed a numerical method to determine the spectra and the rotational temperature of OH-radical. We have normalized the entire spectrum relative to the intensity of the head of the branch  $Q$  and we have used the normalized intensity of the head of the band  $R$  as thermometric function. The Boltzmann's method applied to the normalized intensities of the thermometric stripes  $R$  is used to determine, with the numerical model, the temperatures of rotation of OH-radical. The interest and the originality of the method proposed in this paper is that firstly, it can be used to determine molecular spectra and temperatures of rotation but secondly it can be used also in any medium relatively difficult to diagnose and containing OH-radicals such as industrial sites where the power of resolution of the spectroscopic devices installed is limited. This method also gives an idea on the thermodynamic equilibrium in the medium studied when the Boltzmann representation is not a straight line. The results obtained for all the rotational temperatures are in good agreement with the results of the literature. Then, it is possible to use the results of the spectra to determine the porosity of a medium, the velocity of the particles, etc. Supplementary studies should be desirable in the future taking into account a wide spectral range of wavelength for a wide variety of compounds.

## References

- [1] Müller R, Salawitch RJ. Upper stratospheric processes. In Scientific Assessment of Ozone Depletion: 1998, Albritton DL, ed. World Meteorological Organization, 1999.
- [2] Mills FP, Cageao RP, Sander SP, Allen M, Yung YL, Remsberg EE, Russell JM III, Richter U. OH column abundance over Table Mountain Facility, California: intra- annual variations and comparisons to model predictions for 1997–2001. *J. Geophys. Res.* (2003) 108(D24): 4785, [doi:10.1029/2003JD003481](https://doi.org/10.1029/2003JD003481).
- [3] Pickett HM, Peterson DB. Comparison of measured stratospheric OH with prediction. *J. Geophys. Res.* (1996) 101, 16789–16796.
- [4] Conway RR, Stevens MH, Cardon JG, Zasadil SE, Brown CM, Morrill JS, Mount GH. Satellite measurements of hydroxyl in the mesosphere. *Geophys. Res. Lett.* (1996) 23, 2093–2096.
- [5] Conway RR, Stevens MH, Brown CM, Cardon JG, Zasadil SE, Mount GH. Middle Atmosphere High Resolution Spectrograph Investigation. *J. Geophys. Res.* (1999) 104, 16327–16348.
- [6] Drouin BJ. Isotopic Spectra of the Hydroxyl Radical. Jet Propulsion Laboratory, California Institute of Technology, 4800 Oak Grove Avenue, Pasadena, California 91109, United States, *J. Phys. Chem. A* (2013) 117, 10076–1009.
- [7] Carpentier Y, Pino T, Bréchnignac P. R2PI Spectroscopy of Aromatic Molecules Produced in an Ethylene-Rich Flame. *J. Phys. Chem. A* (2013) 117, 10092–10104.

- [8] Tanner CM, Quack M, Schmidiger D. Nuclear Spin Symmetry Conservation and Relaxation in Water ( $^1\text{H}_2^{16}\text{O}$ ) Studied by Cavity Ring-Down (CRD) Spectroscopy of Supersonic Jets. *J. Phys. Chem. A* (2013) 117, 10105–10118.
- [9] Buckingham GT, Chang CH, Nesbitt DJ. High-Resolution Rovibrational Spectroscopy of Jet-Cooled Phenyl Radical: The  $\nu_{19}$  Out-of-Phase Symmetric CH Stretch. *J. Phys. Chem. A* (2013) 117, 10047–10057.
- [10] Dehghani ZT, Ota S, Mizoguchi A, Kanamori H. Millimeter-Wave Spectroscopy of  $\text{S}_2\text{Cl}_2$ : A Candidate Molecule for Measuring Ortho–Para Transition. *J. Phys. Chem. A* (2013) 117, 10041–10046.
- [11] Siller BM, Hodges JN, Perry AJ, McCall BJ. Indirect Rotational Spectroscopy of  $\text{HCO}^+$ . *J. Phys. Chem. A* (2013) 117, 10034–10040.
- [12] Sun M, Wu Y, Li J, Wang NH, Wu J, Shang KF, Zhang JL. Diagnosis of OH Radical by Optical Emission Spectroscopy in Atmospheric Pressure Unsaturated Humid Air Corona Discharge and its Implication to Desulphurization of Flue Gas. *Plasma Chemistry and Plasma Processing* (2005) 25, 31–40.
- [13] Sprague MK, Mertens LA, Widgren HN, Okumura M. Cavity Ringdown Spectroscopy of the Hydroxy-Methyl-Peroxy Radical. *J. Phys. Chem. A* (2013) 117, 10006–10017.
- [14] Koucký J, Kania P, Uhlíková T, Kolesníková L, Beckers H, Willner H, Urban S. Geometry and Microwave Rotational Spectrum of the  $\text{FC}^{16}\text{O}^{18}\text{O}^{\bullet}$  Radical. *J. Phys. Chem. A* (2013) 117, 10138–10143.
- [15] Turbiner AV, Lopez Vieyra JC. Ground State of the  $\text{H}_3^+$  Molecular Ion: Physics Behind. *J. Phys. Chem. A* (2013), 117, 10119–10128.
- [16] Ouoba S. Etude spectroscopique moléculaire des molécules diatomiques : Cas de OH. Diplôme d'études approfondies de l'université de Ouagadougou, Burkina Faso (2004) pp. 43.
- [17] Koulidiati J. Etude spectroscopique des molécules carbonées diatomiques. Application au diagnostic des plasmas d'hydrocarbures. Thèse de doctorat, université d'Orléans, France (1991) pp. 169.
- [18] Wang W, Wang S, Liu F, Zheng W, Wang D. Optical study of OH radical in a wire-plate pulsed corona discharge. *Spectrochimica Acta Part A* (2006) 63, 477-482.